

## Overcoming the forest-effect in probing the Weibel-instability-generated electric and magnetic fields from proton radiography

Bao Du, Hong-Bo Cai, Wen-Shuai Zhang, Jing Chen and Shao-Ping Zhu  
Institute of Applied Physics and Computational Mathematics, Beijing, China  
E-mail: dubao89@mail.usc.edu.cn

The Weibel instability (WI) is a subject of relevance from many physics fields ranging from ICF to astrophysical scenarios. In two counterstreaming plasma flows, WI can be unstable and lead to stochastically distributed current filaments. The self-generated magnetic field  $\mathbf{B}$  and electric field  $\mathbf{E}$  are the major media by which WI has an impact on the plasma energy transportation, the collisionless shock formation and the gamma ray bursts. Experimentally, WI is usually probed with the side-on proton radiography. The proton density perturbation striations on the detection plane are used to indicate the emergence of WI. However, observations conflict with the assumption that the deflection from  $\mathbf{E}$  is ignorable in the proton radiography [1]. The nature of the radiographed fields has never been carefully examined. Meanwhile, because of the “forest-effect”, deflection from these fields would be compensated by itself, both for  $\mathbf{E}$  and  $\mathbf{B}$ . The proton flux density perturbation  $\delta n/n_0$  can only deliver a qualitative characteristic of the 2D isotropic and stochastic self-generated fields. The strength and spatial wavelength of these fields, which are the most important parameters for WI, remain undetectable. The quantitative diagnostics of  $\mathbf{E}$  and  $\mathbf{B}$  rely on the inversion algorithms, which are still awaiting for developing.

With the new diagnosing methods demonstrated in our work, the compensation of the stochastic fields in the proton radiography of WI is overcome. It allows to overcome the forest-effect extract the strengths and wavelengths of the  $\mathbf{E}$  and  $\mathbf{B}$  from the proton radiography for the first time.

With 3D PIC simulations,  $\mathbf{E}$  and  $\mathbf{B}$  are generated in two counterstreaming plasmas ( $1.1 \times 10^{23}/\text{m}^3$ ,  $\pm 0.5c$ ) [2]. The distributions at about saturation show typical 2D isotropic and stochastic distributions. The proton radiography is calculated with the ray tracing method.

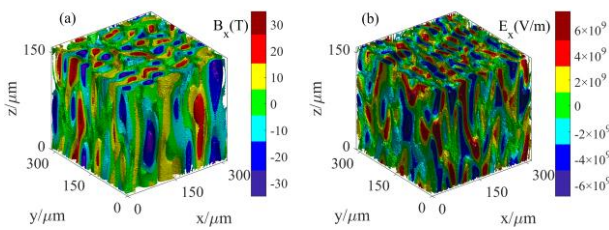


Fig. 1. 3D structures of WI generated  $\mathbf{E}$  and  $\mathbf{B}$ .

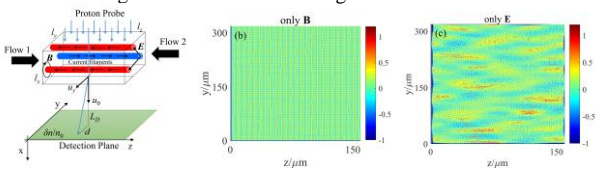


Fig. 2. Proton radiography of the WI.  $\delta n/n_0$  from  $\mathbf{B}$  is much smaller than  $\mathbf{E}$ .  $L_D$  is the detector distance,  $u_0$  is the initial speed of the probe proton beam,  $d$  is the deflection distance.

Country to the traditional assumptions [2], Fig. 2 indicates that the deflection velocity  $u_y$  introduced from  $\mathbf{B}$  is ignorable because of the tube-like structure of  $\mathbf{B}$ .  $\mathbf{E}$  dominates over  $\mathbf{B}$  in deflecting the probe beam in the proton radiography of WI.

By theoretically analyzing the autocorrelation of the 2D isotropic and stochastic  $\mathbf{E}$ , it is found that the energy spectrum of  $\mathbf{E}$  is linked with the spatial spectrum of  $u_y$ ,

$$\varepsilon_E(k_y) = (4\pi/l_x l_y)(\gamma m_p u_0/q)^2 k_y \hat{u}_y^2(k_y) \quad (1)$$

After reconstructing  $u_y$  by  $u_y = -(u_0/L_D) \int_{y_0}^y \delta n/n_0 dy$ , the

strength of  $\mathbf{E}$  is deduced with  $E_{rms}^2 = \int_0^\infty dk \varepsilon_E(k_y)$ , whereas the wavelength  $\lambda_{|E|}$  can be read from  $\varepsilon_E(k)$ . At the same time, after the linear growth stage of WI,  $\mathbf{E}$  is balanced by the magnetic pressure, i.e.,  $\mathbf{E} = -\nabla B^2 / e\mu_0 n_e$  [3]. This allows us to extract the strength and wavelength of  $\mathbf{B}$  from the proton radiography by  $B_{rms} \approx \sqrt{4e\mu_0 n_e E_{rms} \lambda_{|E|} / \pi^2}$  and

$$\lambda_{|B|} = 2\lambda_{|E|}.$$

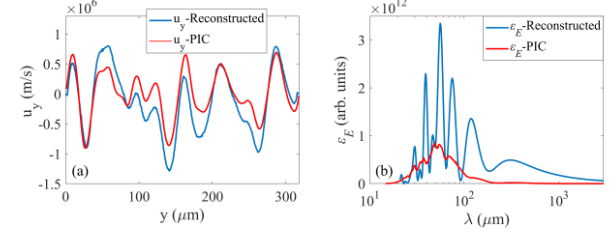


Fig. 3. Comparisons between the reconstructed and simulated  $u_y$ ,  $\varepsilon_E$ .

For  $\mathbf{E}$ , the reconstructed and simulated average strengths  $E_{rms}$  are  $4.1 \times 10^9$  V/m and  $3.1 \times 10^9$  V/m, whereas the wavelengths  $\lambda_{|E|}$  are 28  $\mu\text{m}$  and 24  $\mu\text{m}$ , respectively. For  $\mathbf{B}$ , the reconstructed and simulated average strengths  $B_{rms}$  are 32 T and 18 T, whereas the wavelengths  $\lambda_{|B|}$  are 56  $\mu\text{m}$  and 32  $\mu\text{m}$ , respectively. The consistence between the reconstructed and simulated values validates that the “forest-effect” is overcome with our diagnosing method.

As a comparison, when reconstructed through the traditional  $E_y = \gamma m_p u_0^2 d_s / qL_D l_x$  [4] by reading the striations distances, it gives  $E_{rms} = 4.2 \times 10^{10}$  V/m, which is over one amplitude larger than the PIC simulation. When using the reconstructed  $u_y$  in Fig. 3(a), it gives an average strength of  $\mathbf{E}$  about  $0.7 \times 10^9$  V/m, which is also too small because of the forest-effect. This highlights the advantages of our methods.

### References:

- [1] *Nat. Phys.* **11**, 173 (2015);
- [2] *Phys. Plasmas* **10**, 1979 (2003);
- [3] *Plasma Phys. Control. Fusion* **51**, 124042 (2009);
- [4] *Phys. Rev. Lett.* **97**, 135003 (2006).